DIGITAL ACCESS TO SCHOLARSHIP AT HARVARD
DASH.HARVARD.EDU

HARVARD LIBRARY
Office for Scholarly Communication

Angiotensin II drives the production of tumor-promoting macrophages

Citation

Cortez-Retamozo, Virna, Martin Etzrodt, Andita Newton, Russell Ryan, Ferdinando Pucci, Selena W. Sio, Wilson Kuswanto, et al. 2013. “Angiotensin II Drives the Production of Tumor-Promoting Macrophages.” Immunity 38 (2): 296–308. https://doi.org/10.1016/j.immuni.2012.10.015.

Permanent link
http://nrs.harvard.edu/urn-3:HUL.InstRepos:41384331

Terms of Use
This article was downloaded from Harvard University’s DASH repository, and is made available under the terms and conditions applicable to Other Posted Material, as set forth at http://nrs.harvard.edu/urn-3:HUL.InstRepos:dash.current.terms-of-use#LAA

Share Your Story
The Harvard community has made this article openly available.
Please share how this access benefits you. Submit a story .

Accessibility

NIH Public Access

Author Manuscript

Immunity. Author manuscript; available in PMC 2014 February 21.

Published in final edited form as:

Immunity. 2013 February 21; 38(2): 296–308. doi:10.1016/j.immuni.2012.10.015.

Angiotensin II drives the production of tumor-promoting macrophages

Virna Cortez-Retamozo[1,†], **Martin Etzrodt**[1,†], **Andita Newton**[1], **Russell Ryan**[2], **Ferdinando Pucci**[1], **Selena W. Sio**[1], **Wilson Kuswanto**[1], **Philipp J. Rauch**[1], **Aleksey Chudnovskiy**[1], **Yoshiko Iwamoto**[1], **Rainer Kohler**[1], **Brett Marinelli**[1], **Rostic Gorbatov**[1], **Gregory Wojtkiewicz**[1], **Peter Panizzi**[1], **Mari Mino-Kenudson**[2], **Reza Forghani**[1], **Jose-Luiz Figueiredo**[1], **John W. Chen**[1], **Ramnik Xavier**[3], **Filip K. Swirski**[1], **Matthias Nahrendorf**[1], **Ralph Weissleder**[1,4], and **Mikael J. Pittet**[1,*]

[1]Center for Systems Biology, Massachusetts General Hospital and Harvard Medical School, Boston, MA 02114

[2]Department of Pathology, Massachusetts General Hospital, Boston, MA 02114

[3]Center for Computational and Integrative Biology and Gastrointestinal Unit, Massachusetts General Hospital and Harvard Medical School, Boston, MA 02114

[4]Department of Systems Biology, Harvard Medical School, Boston, MA 02115

SUMMARY

Macrophages frequently infiltrate tumors and can enhance cancer growth, yet the origins of the macrophage response are not well understood. Here we address molecular mechanisms of macrophage production in a conditional mouse model of lung adenocarcinoma. We report that over-production of the peptide hormone Angiotensin II (AngII) in tumor-bearing mice amplifies self-renewing hematopoietic stem cells (HSCs) and macrophage progenitors. The process occurred in the spleen but not the bone marrow, and was independent of hemodynamic changes. The effects of AngII required direct hormone ligation on HSCs, depended on $S1P_1$ signaling, and allowed the extramedullary tissue to supply new tumor-associated macrophages throughout cancer progression. Conversely, blocking AngII production prevented cancer-induced HSC and macrophage progenitor amplification and thus restrained the macrophage response at its source. These findings indicate that AngII acts upstream of a potent macrophage amplification program and that tumors can remotely exploit the hormone's pathway to stimulate cancer-promoting immunity.

INTRODUCTION

Macrophages are tissue-resident white blood cells that protect against infection and injury. Some macrophages, however, inversely affect prognosis by contributing to cancer. Macrophages that infiltrate the tumor stroma are often referred to as tumor-associated macrophages (TAMs). Experimental models using mice have shown that TAMs can

---

© 2013 Elsevier Inc. All rights reserved.

[*]To whom correspondence should be addressed. mpittet@mgh.harvard.edu.

[†]Contributed equally

Additional experimental procedures are included in Supplementary Materials.

Publisher's Disclaimer: This is a PDF file of an unedited manuscript that has been accepted for publication. As a service to our customers we are providing this early version of the manuscript. The manuscript will undergo copyediting, typesetting, and review of the resulting proof before it is published in its final citable form. Please note that during the production process errors may be discovered which could affect the content, and all legal disclaimers that apply to the journal pertain.

facilitate tumor progression by promoting inflammation, stimulating angiogenesis, enhancing tumor cell migration and metastasis, and suppressing anti-tumor immunity (De Palma et al., 2007; Mantovani et al., 2008; Grivennikov et al., 2010; Qian and Pollard, 2010; Hanahan and Coussens, 2012). Clinical studies have further reported that the presence of TAMs correlates with adverse outcome and shorter survival in various cancer types, including non-small-cell lung cancer (NSCLC) (Zhang et al., 2011a; Zhang et al., 2011b); breast cancer (Denardo et al., 2011); and Hodgkin's lymphoma (Steidl et al., 2010). TAMs are often the most abundant host cell population within the tumor stroma, but because they are short-lived and do not proliferate *in situ,* TAMs must be continuously replaced throughout cancer progression (Sawanobori et al., 2008; Movahedi et al., 2010; Cortez-Retamozo et al., 2012).

Inflammatory tissue macrophages descend from circulating monocytes, which are initially produced in bone marrow by hematopoietic stem cells (HSCs) (van Furth and Cohn, 1968; Geissmann et al., 2010). These macrophages are distinct from Myb-independent macrophages that develop in the embryo before the appearance of HSCs (Schulz et al., 2012). Monocyte production by HSCs involves the generation of discrete cell progenitor intermediates, including macrophage and dendritic cell progenitors (MDPs) (Fogg et al., 2006). These hematopoietic stem and progenitor cells (HSPCs) can divide, whereas monocytes and macrophages do not (van Furth and Cohn, 1968). Thus, the prevailing model of macrophage response implies that fundamental amplification and differentiation occur in the bone marrow.

Despite the prevalence of this linear model of macrophage production, HSPCs constitutively exit the bone marrow (Goodman and Hodgson, 1962; Wright et al., 2001) and, during inflammation, support myelopoiesis in extramedullary tissue (Massberg et al., 2007). The spleen's red pulp can be a site of HSPC activity during disease in both humans and mice (Freedman and Saunders, 1981; Cortez-Retamozo et al., 2012; Dutta et al., 2012). The newly produced cells supplement a reservoir of splenic monocytes (Swirski et al., 2009), which are readily mobilized to contribute large numbers of macrophages to distant lesions. This process occurs after myocardial infarction (Leuschner et al., 2012) and during the progression of atherosclerosis (Robbins et al., 2012) and cancer (Cortez-Retamozo et al., 2012). Although the bone marrow maintains the monocyte repertoire in steady state, the monocyte production can be outsourced during inflammatory diseases.

Cancer-induced extramedullary monocytopoiesis promotes generation of cells with heightened tumor-promoting functions (Cortez-Retamozo et al., 2012; Ugel et al., 2012); however, the molecular mechanisms that drive such response remain largely unknown. We investigated the macrophage response using a conditional genetic mouse model of lung adenocarcinoma (hereafter referred to as KP). This model produces autochtonous tumors from a few somatic cells via Cre-recombinase activation of oncogenic Kras and inactivation of p53 (Dupage et al., 2009). Tumors in KP mice present genetic alterations that are frequently found in the human disease, progress to high-grade tumors, and are chronically infiltrated by tumor-promoting macrophages. KP mice thus provide an opportunity to study the macrophage response under *in vivo* conditions that mirror central aspects of the human disease. Our KP mice studies showed that increased AngII augments the production of splenic HSPCs and consequently facilitates TAM supply from extramedullary tissue throughout cancer progression.

RESULTS

AngII amplifies HSCs and macrophage progenitors in the spleen

We investigated AngII because it interacts with mononuclear phagocytes and promotes inflammation (AbdAlla et al., 2004; Lanz et al., 2010; Ma et al., 2012), and because it is found at increased concentrations in the plasma of lung-tumor-bearing KP animals as compared to age-matched tumor-free controls (Fig 1A). AngII is known to release monocytes from their splenic reservoir (Swirski et al., 2009; Shi and Pamer, 2011) and therefore may not be involved in *de novo* mononuclear phagocyte production. Yet splenocytes obtained from mice infused for 1 week with AngII showed elevated colony-forming unit-macrophage (CFU-M) activity *in vitro* (Fig 1B–C). These tumor-free mice received AngII continuously via osmotic mini-pumps at a dose that replicated the plasma concentration found in tumor-bearing mice (Fig 1A). AngII-treated mice and tumor-bearing KP mice showed comparable splenic CFU-M activity (Fig 1B–C). These data led us to consider that AngII may drive splenic macrophage progenitor amplification.

To address AngII's role in amplifying macrophage progenitors, we quantified HSPCs *ex vivo* by flow cytometry in various mouse cohorts. The analyses confirmed a marked increase in total number of splenic Lin^{lo} $\mathrm{CD117}^{+}$ $\mathrm{Sca\text{-}1}^{+}$ HSCs and Lin^{lo} $\mathrm{CD117}^{+}$ $\mathrm{Sca\text{-}1}^{-}$ $\mathrm{CD115}^{+}$ $\mathrm{CD16/32}^{+}$ $\mathrm{CD34}^{+}$ MDPs in AngII-treated mice as compared to control mice (9±1 and 25±4 fold increase for HSCs and MDPs, respectively; Fig 1D, Fig S1A). We observed similar splenic HSC and MDP responses in tumor-bearing KP mice (HSCs: 7±2 fold increase in KP mice compared to control tumor-free mice; MDPs: 20±6 fold increase). These responses remained detectable at week 21 after tumor initiation (Fig S1B).

AngII-treated mice (Fig 1E) and KP tumor-bearing mice (not shown) also expanded splenic common myeloid progenitors (CMPs) and granulocyte macrophage progenitors (GMPs), which are cell intermediates that derive from HSCs and produce MDPs. AngII infusion did not seem to affect other splenic lineages in this experimental setting (Fig 1D). The amplification of HSCs, CMPs, GMPs, MDPs occurred in the spleen but not in bone marrow (Fig 1D, E). Finally, these cell populations were not amplified in the spleens of control mice that received osmotic mini-pumps delivering PBS only (Fig 1E). Thus, AngII alone is sufficient to trigger extramedullary macrophage progenitor amplification as found in tumor-bearing KP mice.

AngII amplifies HSCs and macrophage progenitors regardless of hemodynamics

Tumor development in KP mice did not measurably alter blood pressure (Fig S1C), suggesting that increased AngII levels in these mice did not alter hemodynamics. Nevertheless, because AngII is a known vasoconstrictor, we measured its capacity to induce hematopoietic progenitor cell expansion in the presence of the vasodilator hydralazine. Both AngII and hydralazine were continuously released by osmotic mini-pumps implanted separately in the same animals. Hydralazine treatment reduced systolic and diastolic blood pressures as expected (from 120±14/91±16 to 99±9/65±15 mmHg, mean±SD); however, it did not alter splenic HSC/MDP amplification (Fig 1D). Thus AngII triggers a splenic HSC and macrophage progenitor response independently from its effects on hemodynamics.

Direct AngII-AGTR1A signaling on HSCs and macrophage progenitors

Based on the above results, we investigated whether the hormone acts directly on hematopoietic cells. To test this hypothesis we first generated mouse chimeras in which expression of the AngII receptor, AGTR1A, was restricted to either hematopoietic or non-hematopoietic cells (Fig 2A) and then measured the AngII's capacity to amplify HSCs and MDPs in these mice. The experiments showed that the splenic response depended strictly on

NIH-PA Author Manuscript NIH-PA Author Manuscript NIH-PA Author Manuscript

AngII-AGTR1A signaling in hematopoietic cells (Fig 2B). Furthermore, splenic HSCs and MDPs were amplified equally in mice with *Agtr1a*$^{-/-}$ or *Agtr1a*$^{+/+}$ non-hematopoietic cells (Fig 2B), indicating that AngII-AGTR1A signaling in non-hematopoietic cells did not influence the hematopoietic response.

In a second approach, we tracked *Agtr1a*$^{+/+}$ and *Agtr1a*$^{-/-}$ (EGFP^{+}) HSCs following adoptive transfer into wild-type mice that were infused with AngII. Intravital microscopy of the spleen's red pulp (Pittet and Weissleder, 2011) indicated that donor *Agtr1a*$^{-/-}$ HSCs failed to produce splenic colonies *in vivo* as compared to their *Agtr1a*$^{+/+}$ counterparts (Fig 2C–D and Fig S2). This impairment was not due to an intrinsic proliferative and/or survival defect of *Agtr1a*$^{-/-}$ HSCs because both *Agtr1a*$^{-/-}$ and *Agtr1a*$^{+/+}$ HSCs were equally able to proliferate and produce colonies *in vitro* (Fig 2E), and the few *Agtr1a*$^{-/-}$ HSCs that accumulated in splenic tissue produced colonies that were comparable in average size to the ones produced by *Agtr1a*$^{+/+}$ cells (Fig 2F).

Finally, we used flow cytometry to investigate the fate of transferred HSCs in recipient mice exposed to AngII. In these experiments HSCs and recipient mice were either *Agtr1a*$^{-/-}$ or *Agtr1a*$^{+/+}$ (Fig 2G). Donor *Agtr1a*$^{-/-}$ HSCs failed to produce monocytic cells (defined as CD11b^{+} Ly-6C^{hi} [B220, CD19, CD90.2, DX5, NK1.1, Ly-6G, F4/80, CD11c]^{lo}), whereas *Agtr1a*$^{+/+}$ HSCs efficiently engendered a monocytic progeny even in *Agtr1a*$^{-/-}$ recipient animals. From these experiments, we concluded that: a) HSCs sense AngII directly; b) the HSC response does not depend on AngII-AGTR1A signaling in non-hematopoietic cells; and c) this sensing mechanism amplifies a macrophage progenitor response *in vivo*.

AngII signaling alters *in vivo* trafficking of splenic HSCs

We considered that the hormone might amplify splenic HSCs and macrophage progenitors by inducing them to proliferate; however, analyses conducted both *ex vivo* (Fig 3A) and *in vitro* (Fig S3A) excluded this possibility. Alternatively, the hormone could retain HSPCs that travel through extramedullary tissue (Wright et al., 2001). To test this hypothesis, we established parabiosis between two AngII-infused mice (or two control mice) until splenic HSC equilibration (Massberg et al., 2007) and then measured chimerism of parabiont-derived splenic HSCs after separating the parabionts. The separation prevents further cell exchange between animals; thus, new cells that accumulate in the spleen predominantly originate from the host, and the relative amount of parabiont-derived HSCs that remain in the tissue indicates their residence time (Liu et al., 2007). This experimental approach showed that exposure to AngII significantly increases the retention of HSCs in the spleen (Fig 3B). We then investigated splenic HSC retention in tumor-bearing KP mice. This involved parabiosis between two KP mice (or two control mice) and measuring chimerism using the method detailed above. This experiment further indicated that KP cancer increases splenic HSC retention (Fig 3C). We thus concluded that both AngII and cancer alter splenic HSC trafficking *in vivo*.

AGTR1A ligation alters S1P$_1$ signaling in HSCs

Our next goal was to define how AngII signaling favors retention of HSCs and macrophage progenitors in the spleen. We investigated signaling through Sphingosine-1-Phosphate Receptor 1 (S1P$_1$, also referred to as S1PR1) because this G⟨i-coupled receptor is known to promote HSC recirculation (Massberg et al., 2007). We confirmed that HSCs and macrophage progenitors—but not monocytes—expressed *S1p1* at detectable levels in steady state (Fig S3B); however, these cells strongly repressed *S1p1* expression in mice exposed to AngII (Fig 3E). Furthermore, HSCs failed to down-regulate *S1p1* expression in *Agtr1a*$^{-/-}$ mice exposed to AngII *in vivo* (Fig 3D), and purified HSCs subjected to AngII *in vitro* down-regulated *S1p1* only if they expressed AGTR1A (Fig 3E). These findings indicate that

AngII-mediated repression of *S1p1* in HSCs requires direct signaling through the AGTR1A receptor.

In accordance with the above findings, we found that splenic progenitors obtained from AngII–infused mice (i.e. cells which had down-regulated *S1p1* expression *in vivo*) lost their ability to migrate toward an S1P gradient *ex vivo* (Fig 3F). Control experiments showed that the same cells remained capable of migrating toward the cytokine SDF-1α and thus remained biologically active (Fig S3C). Also, *in vivo* administration of the small-molecule inhibitor FTY720, which impairs S1P sensing by $S1P_1$ (Schwab and Cyster, 2007), was sufficient to promote the accumulation of HSCs in the spleen (Fig 3G).

We then assessed whether the splenic hematopoietic response mediated by AngII indeed depends on $S1P_1$ signaling. To this end, we engineered both *S1p1*^{const} *CD45.1*$^{+}$ *EGFP*$^{+}$ HSCs (i.e. HSCs that expressed $S1P_1$ constitutively and were tracked according to CD45.1 and EGFP expression) and *S1p1*^{norm} *CD45.2*$^{+}$ *EGFP*$^{+}$ HSCs (i.e. HSCs that could down-regulate $S1P_1$ normally and were tracked according to CD45.2 and EGFP expression). We used a competitive assay to test these two HSC populations' capacity to produce monocytic cells in response to AngII *in vivo*. Specifically, equal numbers of the two HSC populations were co-injected into EGFP^{-} recipient mice, which were infused with AngII. The monocyte progeny of donor EGFP^{+} HSCs were analyzed 7 d later by flow cytometry (Fig 3H). *S1p1*^{norm} HSC-derived monocytes outnumbered their *S1p1*^{const} counterparts by ~4:1, indicating that AngII-mediated *S1p1* down-regulation in HSCs directly amplifies monocytes *in vivo* (Fig 3I–J).

Splenic HSCs decreased *S1p1* expression in tumor-bearing KP mice as expected (Fig 3K); however, administering either the AGTR1A antagonist losartan or the Angiotensin converting enzyme inhibitor enalapril (used to decrease AngII levels) prevented this process (Fig 3K). Based on these findings, we investigated whether reducing AngII production in KP mice by injecting enalapril could prevent cancer-induced HSC and macrophage progenitor amplification and thus restrain the TAM response.

Blocking AngII production impairs the TAM response at its source

Initially, we analyzed KP mice at 12 wk after tumor initiation and 5 d after reducing AngII production with enalapril (Fig 4A). In this experimental setting, temporarily interrupting AngII production did not detectably affect tumor burden (not shown) but did restrain the amplification of splenic HSCs and HSC-derived MDPs, monocytes, and lung macrophages (Fig 4B). Lung macrophages were defined as F4/80^{+} [B220, CD19, CD90.2, DX5, NK1.1, Ly-6G]$^{-/lo}$. These cells express CD11b at varying levels (Cortez-Retamozo et al., 2012).

In a second approach, we transferred donor EYFP^{+} hematopoietic progenitor cells into cohorts of recipient animals in order to evaluate the capacity of a discrete cell population to produce TAMs in different *in vivo* conditions (Fig 4C). Analysis by flow cytometry on d 5 post transfer showed that donor progenitor cells produced splenic monocytes and TAMs in tumor-bearing KP mice, as expected (Fig 4D). However, enalapril administration in KP mice decreased the production of these cells to levels found in tumor-free controls (Fig 4D).

We further investigated enalapril's impact on the TAM response by artificially limiting the drug's action to the spleen. Specifically, EYFP^{-} recipient KP mice (not treated with enalapril) received spleens transplanted from EYFP^{+} KP donor mice, some of which that were previously treated with enalapril (Fig 4E). The procedure allowed us to track EYFP^{+} splenocytes that relocated into the recipient (Swirski et al., 2009). Donor spleens were extensively perfused before transplantation to avoid exposing recipient mice to the drug. Analysis at 24 h post transplantation showed that enalapril-treated spleens contributed significantly fewer EYFP$^+$ TAMs than their control counterparts (Fig 4F). Taken together, the above findings indicate that short-term blockade of AngII production restrains TAM progenitor amplification in the spleen. Furthermore, enalapril treatment likely did not trigger direct anti-tumor effects in KP mice because tumor cells derived from these mice remained fully able to expand in presence of high dose enalapril *in vitro* (Fig S4).

Prolonged reduction of AngII production restrains TAMs and increases survival

Following the short-term results reported above, we investigated the impact of uninterrupted, extended enalapril treatment of KP mice. KP mice received daily enalapril over 3 wk starting at wk 8 after tumor initiation. This dose is well tolerated *in vivo* (Leuschner et al., 2010). Controls included untreated KP mice, KP mice that received hydralazine (to monitor the effects of low blood pressure triggered by enalapril treatment), and tumor-free controls. Evaluation in wk 11 showed that enalapril treatment restrained tumor-induced HSC and MDP responses in the spleen but not in bone marrow, whereas treatment with hydralazine had no effect (Fig 5A). Enalapril, but not hydralazine, also compromised downstream monocyte amplification in the spleen and macrophage accumulation in the lungs (Fig 5B, Fig S5A–B).

The lung macrophage repertoire comprises cells that derive from HSC-independent precursors (Schulz et al., 2012) and Ly-6C^{lo} monocytes (Landsman et al., 2007)—these macrophages are found already in steady-state—as well as Ly-6C^{hi} monocytes that accumulate in diseased lung during tumor development. Accordingly, lung macrophages were qualitatively different in tumor-bearing and tumor-free mice (Fig 5C). Over-expression of several of the transcripts found at higher levels in macrophages from tumor-bearing mice is associated with the acquisition of tumor-promoting functions (Gabrilovich et al., 2012). Treatment of tumor-bearing mice with enalapril largely restored the lung macrophage phenotypes to that observed in tumor-free mice (Fig 5C). These results suggest that enalapril treatment in KP mice prevents accumulation of Ly-6C^{hi} monocyte-derived, tumor-promoting macrophages.

To evaluate the impact of enalapril and hydralazine on tumor progression, we used high-resolution computed tomography (CT) to image the lungs of KP mice 11 wk after tumor induction (i.e. 3 wk after starting enalapril or hydralazine treatments). This experiment showed that enalapril treatment restrained the number of detectable lung tumor nodules and total lung tumor volumes in the majority of mice analyzed, whereas control mice treated with hydralazine showed full-fledged tumor progression (Fig 5D–E). Histopathological analysis on wk 11 confirmed that enalapril treatment reduced cancer growth (Fig S5C).

Next we performed a 30-week longitudinal study to compare the survival of KP mice that received either no treatment or enalapril alone. Kaplan-Meier analysis indicated that treatment with 50 mg/kg enalapril increased survival (p=0.0038, Mantel-Cox test; Fig 5E). The phenotype was preserved in a separate experiment in which mice received a lower dose of enalapril (5 mg/kg; p=0.031, Mantel-Cox test). Collectively, these findings indicate that targeting the AngII pathway restrains macrophage progenitor amplification, reduces the number of TAMs and provides therapeutic benefit in the KP mouse model.

AGT over-expression in mouse and human NSCLC

To begin to explore what mechanisms control AngII production in KP mice, we examined expression levels of angiotensinogen (Agt), the AngII precursor normally produced in the liver. Interestingly, we found significant Agt over-expression in the lungs of tumor-bearing mice (6.6±1.8 mean fold increase when compared to control lungs from). Agt expression was selectively increased in tumor-involved regions, both at transcript (Fig 6A) and protein

NIH-PA Author Manuscript NIH-PA Author Manuscript NIH-PA Author Manuscript

(Fig 6B) levels. Analyzing tumor stroma cell fractions (tumor cells, macrophages and others) suggested that tumor cells are a major source of Agt (Fig S6A). We confirmed that Agt was produced by at least some carcinoma cells: 4/13 tumor cell lines derived from KP tumor nodules still over-expressed Agt *in vitro* (Fig S6B). By comparison, other candidate factors that may influence the macrophage response (*Csf1, Csf2, Ifng, Il1b and Tnfa*) did not detectably increase in tumor-involved regions (Fig S6C). KP tumor nodules excised and cultured *in vitro* produced AngII in supernatant (Fig S6D), suggesting that at least a fraction of Agt produced by tumors may be converted into AngII locally.

Evaluating mouse and human NSCLC cell lines indicated that tumors can produce and secrete Agt at comparable levels in both species (Fig S6E). We also assessed Agt in 44 human NSCLC biopsies and identified 16 specimens in which the peptide was over-expressed (see representative samples in Fig 6C). 13 of the 16 were additionally stained with macrophage markers and all showed marked infiltration by $CD68^+CD163^+$ TAMs (Fig S6F). CD163 expression by TAMs suggests that these cells have tumor-promoting functions (Biswas and Mantovani, 2010). Additionally, 2 control biopsies showed relatively few $CD68^+CD163^-$ macrophages in uninvolved lung tissue (Fig S6F).

To broaden our analysis, we mined publicly available information. Analyzing 11 mRNA datasets of NSCLC-involved and non-involved human tissue (Oncomine database) confirmed increased *AGT* expression in tumor stroma (p-value: 0.0000274; Fig S6G–H). To evaluate whether *AGT* levels in human patients might be associated with clinical prognosis, we consulted additional databases that provide not only tumor tissue transcriptome profiles at diagnosis but also follow-up clinical information (Nguyen et al., 2009). Patients were operationally separated into two cohorts according to *AGT* expression: patients whose tumors expressed the highest or lowest levels of *AGT*. Kaplan-Meier analysis of these two cohorts suggested increased mortality for those whose tumors initially showed higher *AGT* expression (p=0.0552; Fig S6I). Clinical information available for these patients is provided in Table S1. Finally, evaluating 5 datasets reporting DNA copy numbers (Oncomine database) revealed an *AGT* mean copy number gain in NSCLC-involved tissue (p-value: 0.038; Fig S6J). Such gene amplification might contribute to Agt over-expression in some cases and possibly confer an advantage for disease progression. These data suggest that exploitation of the AngII pathway by tumors is not limited to KP mice but may also occur in a subset of human lung cancer patients. Nonetheless, additional studies are needed to test further the relevance of this pathway in patients.

DISCUSSION

We investigated AngII's effects on macrophage production at the organismal level in mice. Our findings indicate that the hormone directly causes self-renewing HSCs and macrophage progenitors to amplify in the spleen's red pulp. By augmenting these cells, the hormone helps maintain splenic monocyte stores and enables extramedullary tissue to continuously supply new inflammatory macrophages. These results reveal AngII's central role in chronic inflammation mediated by macrophages.

AngII "reprograms" HSPC trafficking by compartmentalizing these cells to the spleen. HSPC sequestration involves suppressing $S1P_1$-S1P signaling, according to this pathway's essential role in controlling leukocyte egress from peripheral lymphoid organs (Schwab and Cyster, 2007; Massberg et al., 2007). We did not observe AngII inducing HSPC accumulation in lymph nodes; this is likely because homing to lymph nodes requires CCR7, which is not expressed by HSPCs (Massberg et al., 2007).

This study also shows that AngII-AGTR1A signaling in KP mice amplifies TAMs. By acting on splenic HSPCs, AngII induces the production of monocytic intermediates which are mostly Ly-6C^{hi}. This subset is known to be recruited efficiently to tumors and to carry mediators that stimulate cancer-associated inflammation and angiogenesis (Movahedi et al., 2010; Cortez-Retamozo et al., 2012). These findings concur with previous observations that the renin-angiotensin system promotes inflammation and angiogenesis in the tumor stroma (George et al., 2010) and suggest that AngII fosters these processes at least partially by sustaining the TAM response.

HSCs express ACE (Jokubaitis et al., 2008), a peptidase that is responsible for conversion of AngI to the principal effector AngII. It has been proposed that ACE promotes the generation of myeloid progenitors in an AGTR1A-dependent manner (Lin et al., 2011) and that AGTR1A signaling controls M-CSFR expression in HSCs (Tsubakimoto et al., 2009). Thus, AngII-AGTR1A signaling may not only promote HSC amplification in the spleen, but also favor local production of mononuclear phagocyte lineage cells.

Whereas AngII amplifies HSPCs and monocytes in the spleen, monocyte recruitment from circulation to tumor stroma is thought to occur mainly via interaction between the chemokine MCP-1 and its receptor CCR2 (Sawanobori et al., 2008; Cortez-Retamozo et al., 2012). This suggests that mononuclear phagocyte production and recruitment to tumors are two distinct processes that are controlled separately. It is also likely that mononuclear phagocytes are produced in absence of AngII under some conditions. Identifying additional long-range signaling pathways that control splenic HSPC amplification and inflammatory monocyte production requires further investigation. Interestingly, however, a plasma proteome profiling study identified increased AGT levels in several genetic mouse models of cancer, including NSCLC driven by KRAS or EGFR (Taguchi et al., 2011), suggesting that diverse cancer types can activate the AngII pathway.

How do mouse and human hematopoietic responses compare? Because lung cancer patients' spleens are typically neither removed nor biopsied, we could not assess whether this type of cancer triggers splenic HSPC amplification in humans. Nevertheless, *ex vivo* analysis of splenic tissue from patients with pancreatic ductal adenocarcinoma indicates not only that human tumors promote extramedullary monocyte production but also that the magnitude of this activity is comparable in humans and mice when scale differences between species are taken into account (Cortez-Retamozo et al., 2012). Similar splenic HSPC responses have been observed in patients with cardiovascular diseases (Dutta et al., 2012). However, the extent to which the human spleen contributes TAMs, and whether ACEi treatment controls extramedullary monocytopoiesis in cancer patients, requires study. Molecular imaging technologies that assess biological processes non-invasively in patients are being developed (Weissleder and Pittet, 2008), and such advances may be used to evaluate the extramedullary macrophage progenitor response in NSCLC or other cancers.

As detailed above, ACEi treatment suppresses TAM progenitor amplification and increases survival in tumor-bearing KP mice. The efficacy of such treatment in at least some human patients requires investigation. Interestingly, a retrospective study by Lever et al. hypothesized that long-term ACEi treatment protects against human cancer based on decreased risk of both incidence of and fatality from lung and breast cancers (Lever et al., 1998). The risk of cancer did not decrease in patients receiving other classes of anti-hypertensive drugs. These results agree with our findings that anti-tumor effects mediated by ACEi depend on mechanisms other than those controlling blood pressure.

Several retrospective evaluations of ACEi or AngII receptor blocker (ARB) treatment on cancer incidence provide different conclusions. One study reported a decreased risk of developing cancer in those receiving ACEi (Lang, 2006). By contrast, another study suggested increased incidence of cancer in patients receiving ARBs (Sipahi et al., 2010), though two subsequent investigations questioned this result and concluded that ACEi and ARB alone neither increases nor decreases cancer incidence (Bangalore et al., 2011), or that ARBs may prevent cancer development (Huang et al., 2011). In addition, it remains to be determined whether ACEi or ARB therapy may benefit patients with established cancer. Addressing these questions requires testing in prospective human clinical trials.

The present study implies that such human trials should consider NSCLC patients in whom the AngII pathway is elevated. Based on increasing evidence that the immune system contributes to cancer progression, research should focus on drug combinations that not only efficiently kill cancer cells but also shape the immune system in a way that is favorable to the host (Zitvogel et al., 2008). ACEi could be used to reduce TAM production in patients that over-express AngII, while other co-administered agents would target tumor cells and possibly other host cell components. A retrospective study of NSCLC patients undergoing first-line platinum-based therapy suggests that either ACEi or ARB therapy may increase survival, yet the survival advantage could not be attributed to other established risk factors (Wilop et al., 2009).

Considering the complex nature of RAS signaling (George et al., 2010), it is possible that distinct therapeutics such as ACEi and ARBs mediate divergent effects on the hematopoietic response. Future studies should compare these two drugs' effects on HSC and macrophage production *in vivo*. It will also be important to consider tumor resistance to ACEi or ARBs following extended treatment, a process that can already be investigated in animal models.

In conclusion, we show that AngII has a profound impact on the macrophage response, that this mechanism fosters cancer growth in KP mice, and that blocking AngII production can restrain macrophage amplification. These data also have important experimental and therapeutic implications that go beyond cancer. For instance, extramedullary HSPC amplification governs the macrophage response in experimental myocardial infarction (Leuschner et al., 2012) and atherosclerosis (Robbins et al., 2012), two inflammatory conditions associated with increased AngII activity in humans (McAlpine and Cobbe, 1988; Schieffer et al., 2000). Future studies should thus explore AngII's capacity to amplify macrophage production in various clinical settings.

EXPERIMENTAL PROCEDURES

Animals and tumor models

$Kras^{LSL-G12D/+};p53^{fl/fl}$ (referred to as *KP*) mice in a 129 background were used as a conditional mouse model of NSCLC and described previously (Cortez-Retamozo et al., 2012). To induce lung adenocarcinoma, KP mice were infected with an adenovirus expressing Cre recombinase (AdCre) by intranasal instillation, as described previously (Dupage et al., 2009). AdCre was purchased from the University of Iowa Gene Transfer Vector Core. For parabiosis and spleen transplant experiments, a murine NSCLC cell line isolated from tumor nodules of KP mice and injected intravenously to induce lung adenocarcinoma. Usually, we injected $0.5–1\times10^5$ tumor cells and mice were analyzed 6–7 week post injection.

(ACTB-eYFP)7AC5Nagy/J (referred to as *EYFP*) mice in a 129 background were a gift from Dr. Andras Nagy, Mount Sinai Hospital, Toronto, Canada. $Agtr1a^{-/-}$ *B6.129P2-Agtr1atm1Unc/J* (referred to as $Agtr1a^{-/-}$) mice, *C57BL/6-Tg (UBC-GFP)30Scha/J* (referred to as *GFP*) mice, *B6.SJL-Ptprca Pepcb/BoyJ* (referred to as *CD45.1*) mice, C57BL/6 mice and 129 mice were bought from The Jackson Laboratory. All animal experiments

were approved by the Massachusetts General Hospital Subcommittee on Research Animal Care.

Flow cytometry and cell sorting

Information about the antibodies used in the study (clone number and vendor) is listed in Supplementary Materials. The number of monocytes / macrophages, progenitor and other cells was defined as the total number of cells per organ multiplied by the percentage of each cell type identified by flow cytometry (LSRII; BD Biosciences). Data were analyzed with FlowJo v.8.8.7 (Tree Star, Inc.). For adoptive transfer experiments, cell suspensions obtained from the spleen or the bone marrow were stained with appropriate antibodies; cells of interest were sorted (FACS Aria, BD Biosciences) and injected intravenously without delay. Typically, 0.3–1×10^5 HSC were injected.

Histology

For histological analysis, mouse lung tissue was harvested, fixed in 10% formalin solution, and embedded in paraffin. Serial paraffin-embedded sections were prepared and the tissue sections were stained with hematoxylin and eosin (H&E) (Sigma Aldrich). Paraffin embedded lung sections from 44 patients with stage 1 lung adenocarcinoma were obtained at Massachusetts General Hospital. A detailed protocol for detection of Agt, CD68 and CD162 in lung tissue is included in Supplementary Materials. All stained human tissue sections were analyzed independently by two trained lung pathologists. Agt staining was scored from 0 to 200 (200 is equivalent to high Agt staining in 100% of tumor cells; 100 is equivalent to high Agt staining in 50% of tumor cells or intermediate staining in 100% of tumor; 0 is equivalent to undetectable Agt staining). Final score for a sample was defined as the mean of the two scores given by the pathologists. The threshold value used to identify samples that over-express AGT was 50, which is equivalent to high staining in 25% of tumor cells or intermediate staining in 50% of tumor cells.

Intravital microscopy

Wild-type or *Agtr1a*$^{-/-}$ GFP$^+$ HSC cells were adoptively transferred to Ang II-treated mice and visualized in the spleen 7 d later using an Olympus FV1000 confocal laser scanning system on an upright BX61-WI microscope running the Fluoview 1000 version 2.1 software (Olympus). For imaging, the mice were placed onto a temperature regulated heating-plate (Olympus Corporation Tokyo, JP) set to 38°C. The spleen was exposed surgically and kept moist during imaging as previously described (Swirski et al., 2009). A 20X Olympus objective (Uplan FL N, NA 0.5) was used for imaging with fields of view of 535 μm. Cells expressing GFP and blood vessels labeled with AngioSense-680 (ViSen Medical-Perkin Elmer) were visualized through excitation at 488 nm and 635 nm, also as previously described (Swirski et al., 2009).

Noninvasive evaluation of tumor burden by high resolution CT

Mice infected with AdCre, and treated or not with ACEi, were anonymized, subjected to high-resolution CT at different time points, and analyzed blindly by a radiologist. Mice were anesthetized with isoflurane gas inhalation. They also had a respiratory pillow placed underneath the abdomen to provide gating of x-ray exposures on expiration of the respiratory cycle and thus to prevent motion artifacts. The CT data were acquired on an Inveon PET-CT system (Siemens; isotropic spatial resolution: 50 μm). For CT imaging, Isovue-370 (Bracco Diagnostics) was infused intravenously at 55 μl/min through a tail vein catheter to increase vascular contrast. For data analysis, multiplanar and 3D reconstructions were obtained using OsiriX (The OsiriX foundation) and AMIRA (Visage Imaging, Inc.).

Tumor number and volume were segmented and measured by two board-certified radiologists who were blinded to the treatment groups and to each other's measurements.

Quantitative real-time PCR

Tissue samples were collected into RNA later solution (Ambion). Homogenization was performed in RLT lysis buffer (Qiagen) supplemented with 1% 2-mercaptoethanol using a glass dounce tissue homogenizer. For FACS sorted cells the populations of interest were collected into RLT buffer directly (350 μl RLT/1×10^5 cells). RNA extraction was performed without delay using the Qiagen RNAeasy mini or micro kits (Qiagen). Complementary DNA was prepared using the High Capacity cDNA Reverse Transcription Kit (Applied Biosystems). The primers and probes that were used are described in Supplementary Materials.

Statistics

Statistical tests included unpaired, 2-tailed Student's t test and 1-way ANOVA followed by Tukey's multiple comparison test (for more than 2 groups). For data not normally distributed, we applied the nonparametric Krustal-Wallis test followed by the Dunn's multiple comparison test. For survival studies we applied the Mantel-Cox test. Demographic and Clinical Characteristics of patients were analyzed by means of the Fisher's exact test, chi-squared and unpaired 2-tailed Student's t test. P values <0.05 were considered to denote significance.

Supplementary Material

Refer to Web version on PubMed Central for supplementary material.

Acknowledgments

The authors thank Jessica Truelove (MGH) for imaging and Michael Waring and Adam Chicoine (Ragon Institute, MGH) for sorting cells. This work was supported in part by NIH grants P50 CA86355, R01-AI084880, R56-AI084880 and MGH-Center for Systems Biology (to M.J.P.) and U54-CA126515 (to R.W.). M.E. is part of the International PhD program 'Cancer and Immunology' at the University of Lausanne, Switzerland, and was supported by the AACR Centennial Predoctoral Fellowship and the Boehringer Ingelheim Fonds.

References

AbdAlla S, Lother H, Langer A, el Faramawy Y, Quitterer U. Factor XIIIA transglutaminase crosslinks AT1 receptor dimers of monocytes at the onset of atherosclerosis. Cell. 2004; 119:343–354. [PubMed: 15507206]

Bangalore S, Kumar S, Kjeldsen SE, Makani H, Grossman E, Wetterslev J, Gupta AK, Sever PS, Gluud C, Messerli FH. Antihypertensive drugs and risk of cancer: network meta-analyses and trial sequential analyses of 324,168 participants from randomised trials. Lancet Oncol. 2011; 12:65–82. [PubMed: 21123111]

Biswas SK, Mantovani A. Macrophage plasticity and interaction with lymphocyte subsets: cancer as a paradigm. Nat Immunol. 2010; 11:889–896. [PubMed: 20856220]

Cortez-Retamozo V, Etzrodt M, Newton A, Rauch PJ, Chudnovskiy A, Berger C, Ryan R, Iwamoto Y, Marinelli B, Gorbatov R, Forghani R, Novobrantseva TI, Koteliansky V, Figueiredo JL, Chen JW, Anderson DG, Nahrendorf M, Swirski FK, Weissleder R, Pittet M. Origins of tumor-associated macrophages and neutrophils. Proc Natl Acad Sci U S A. 2012; 109:2491–2496. [PubMed: 22308361]

De Palma M, Murdoch C, Venneri MA, Naldini L, Lewis CE. Tie2-expressing monocytes: regulation of tumor angiogenesis and therapeutic implications. Trends Immunol. 2007; 28:519–524. [PubMed: 17981504]

Denardo DG, Brennan DJ, Rexhepaj E, Ruffell B, Shiao SL, Madden SF, Gallagher WM, Wadhwani N, Keil SD, Junaid SA, Rugo HS, Hwang ES, Jirstrom K, West BL, Coussens LM. Leukocyte Complexity Predicts Breast Cancer Survival and Functionally Regulates Response to Chemotherapy. Cancer Discov. 2011; 1:54–67. [PubMed: 22039576]

Dupage M, Dooley A, Jacks T. Conditional mouse lung cancer models using adenoviral or lentiviral delivery of Cre recombinase. Nature Protocols. 2009; 4:1064–1072.

Dutta P, Courties G, Wei Y, Leuschner F, Gorbatov R, Robbins CS, Iwamoto Y, Thompson B, Carlson AL, Heidt T, Majmudar MD, Lasitschka F, Etzrodt M, Waterman P, Waring MT, Chicoine AT, van der Laan AM, Niessen HW, Piek JJ, Rubin BB, Butany J, Stone JR, Katus HA, Murphy SA, Morrow DA, Sabatine MS, Vinegoni C, Moskowitz MA, Pittet MJ, Libby P, Lin CP, Swirski FK, Weissleder R, Nahrendorf M. Myocardial infarction accelerates atherosclerosis. Nature. 2012; 487:325–329. [PubMed: 22763456]

Fogg DK, Sibon C, Miled C, Jung S, Aucouturier P, Littman DR, Cumano A, Geissmann F. A clonogenic bone marrow progenitor specific for macrophages and dendritic cells. Science. 2006; 311:83–87. [PubMed: 16322423]

Freedman MH, Saunders EF. Hematopoiesis in the human spleen. Am J Hematol. 1981; 11:271–275. [PubMed: 7053225]

Gabrilovich DI, Ostrand-Rosenberg S, Bronte V. Coordinated regulation of myeloid cells by tumours. Nat Rev Immunol. 2012; 12:253–268. [PubMed: 22437938]

Geissmann F, Manz MG, Jung S, Sieweke MH, Merad M, Ley K. Development of monocytes, macrophages, and dendritic cells. Science. 2010; 327:656–661. [PubMed: 20133564]

George AJ, Thomas WG, Hannan RD. The renin-angiotensin system and cancer: old dog, new tricks. Nat Rev Cancer. 2010; 10:745–759. [PubMed: 20966920]

Goodman JW, Hodgson GS. Evidence for stem cells in the peripheral blood of mice. Blood. 1962; 19:702–714. [PubMed: 13900318]

Grivennikov SI, Greten FR, Karin M. Immunity, inflammation, and cancer. Cell. 2010; 140:883–899. [PubMed: 20303878]

Hanahan D, Coussens LM. Accessories to the crime: functions of cells recruited to the tumor microenvironment. Cancer Cell. 2012; 21:309–322. [PubMed: 22439926]

Huang CC, Chan WL, Chen YC, Chen TJ, Lin SJ, Chen JW, Leu HB. Angiotensin II receptor blockers and risk of cancer in patients with systemic hypertension. Am J Cardiol. 2011; 107:1028–1033. [PubMed: 21256465]

Jokubaitis VJ, Sinka L, Driessen R, Whitty G, Haylock DN, Bertoncello I, Smith I, Peault B, Tavian M, Simmons PJ. Angiotensin-converting enzyme (CD143) marks hematopoietic stem cells in human embryonic, fetal, and adult hematopoietic tissues. Blood. 2008; 111:4055–4063. [PubMed: 17993616]

Landsman L, Varol C, Jung S. Distinct differentiation potential of blood monocyte subsets in the lung. J Immunol. 2007; 178:2000–2007. [PubMed: 17277103]

Lang L. ACE inhibitors may reduce esophageal cancer incidence. Gastroenterology. 2006; 131:343–344.

Lanz TV, Ding Z, Ho PP, Luo J, Agrawal AN, Srinagesh H, Axtell R, Zhang H, Platten M, Wyss-Coray T, Steinman L. Angiotensin II sustains brain inflammation in mice via TGF-beta. J Clin Invest. 2010; 120:2782–2794. [PubMed: 20628203]

Leuschner F, Panizzi P, Chico-Calero I, Lee WW, Ueno T, Cortez-Retamozo V, Waterman P, Gorbatov R, Marinelli B, Iwamoto Y, Chudnovskiy A, Figueiredo JL, Sosnovik DE, Pittet MJ, Swirski FK, Weissleder R, Nahrendorf M. Angiotensin-converting enzyme inhibition prevents the release of monocytes from their splenic reservoir in mice with myocardial infarction. Circ Res. 2010; 107:1364–1373. [PubMed: 20930148]

Leuschner F, Rauch PJ, Ueno T, Gorbatov R, Marinelli B, Lee WW, Dutta P, Wei Y, Robbins C, Iwamoto Y, Sena B, Chudnovskiy A, Panizzi P, Keliher E, Higgins JM, Libby P, Moskowitz MA, Pittet MJ, Swirski FK, Weissleder R, Nahrendorf M. Rapid monocyte kinetics in acute myocardial infarction are sustained by extramedullary monocytopoiesis. J Exp Med. 2012; 209:123–137. [PubMed: 22213805]

Lever AF, Hole DJ, Gillis CR, McCallum IR, McInnes GT, MacKinnon PL, Meredith PA, Murray LS, Reid JL, Robertson JW. Do inhibitors of angiotensin-I-converting enzyme protect against risk of cancer? Lancet. 1998; 352:179–184. [PubMed: 9683206]

Lin C, Datta V, Okwan-Duodu D, Chen X, Fuchs S, Alsabeh R, Billet S, Bernstein KE, Shen XZ. Angiotensin-converting enzyme is required for normal myelopoiesis. FASEB J. 2011; 25:1145–1155. [PubMed: 21148418]

Liu K, Waskow C, Liu X, Yao K, Hoh J, Nussenzweig M. Origin of dendritic cells in peripheral lymphoid organs of mice. Nat Immunol. 2007; 8:578–583. [PubMed: 17450143]

Ma F, Li Y, Jia L, Han Y, Cheng J, Li H, Qi Y, Du J. Macrophage-Stimulated Cardiac Fibroblast Production of IL-6 Is Essential for TGF beta/Smad Activation and Cardiac Fibrosis Induced by Angiotensin II. PLoS One. 2012; 7:e35144. [PubMed: 22574112]

Mantovani A, Allavena P, Sica A, Balkwill F. Cancer-related inflammation. Nature. 2008; 454:436–444. [PubMed: 18650914]

Massberg S, Schaerli P, Knezevic-Maramica I, Köllnberger M, Tubo N, Moseman EA, Huff IV, Junt T, Wagers AJ, Mazo IB, von Andrian UH. Immunosurveillance by hematopoietic progenitor cells trafficking through blood, lymph, and peripheral tissues. Cell. 2007; 131:994–1008. [PubMed: 18045540]

McAlpine HM, Cobbe SM. Neuroendocrine changes in acute myocardial infarction. Am J Med. 1988; 84:61–66. [PubMed: 3064600]

Movahedi K, Laoui D, Gysemans C, Baeten M, Stange G, Van den Bossche J, Mack M, Pipeleers D, In't Veld P, De Baetselier P, Van Ginderachter JA. Different tumor microenvironments contain functionally distinct subsets of macrophages derived from Ly6C(high) monocytes. Cancer Res. 2010; 70:5728–5739. [PubMed: 20570887]

Nguyen DX, Chiang AC, Zhang XH, Kim JY, Kris MG, Ladanyi M, Gerald WL, Massague J. WNT/TCF signaling through LEF1 and HOXB9 mediates lung adenocarcinoma metastasis. Cell. 2009; 138:51–62. [PubMed: 19576624]

Pittet MJ, Weissleder R. Intravital imaging. Cell. 2011; 147:983–991. [PubMed: 22118457]

Qian BZ, Pollard JW. Macrophage diversity enhances tumor progression and metastasis. Cell. 2010; 141:39–51. [PubMed: 20371344]

Reich M, Liefeld T, Gould J, Lerner J, Tamayo P, Mesirov JP. GenePattern 2.0. Nat Genet. 2006; 38(5):500–501. [PubMed: 16642009]

Robbins CS, Chudnovskiy A, Rauch PJ, Figueiredo JL, Iwamoto Y, Gorbatov R, Etzrodt M, Weber GF, Ueno T, van Rooijen N, Mulligan-Kehoe MJ, Libby P, Nahrendorf M, Pittet MJ, Weissleder R, Swirski FK. Extramedullary Hematopoiesis Generates Ly-6Chigh Monocytes that Infiltrate Atherosclerotic Lesions. Circulation. 2012; 125:364–374. [PubMed: 22144566]

Sawanobori Y, Ueha S, Kurachi M, Shimaoka T, Talmadge JE, Abe J, Shono Y, Kitabatake M, Kakimi K, Mukaida N, Matsushima K. Chemokine-mediated rapid turnover of myeloid-derived suppressor cells in tumor-bearing mice. Blood. 2008; 111:5457–5466. [PubMed: 18375791]

Schieffer B, Schieffer E, Hilfiker-Kleiner D, Hilfiker A, Kovanen PT, Kaartinen M, Nussberger J, Harringer W, Drexler H. Expression of angiotensin II and interleukin 6 in human coronary atherosclerotic plaques: potential implications for inflammation and plaque instability. Circulation. 2000; 101:1372–1378. [PubMed: 10736279]

Schulz C, Gomez Perdiguero E, Chorro L, Szabo-Rogers H, Cagnard N, Kierdorf K, Prinz M, Wu B, Jacobsen SE, Pollard JW, Frampton J, Liu KJ, Geissmann F. A lineage of myeloid cells independent of Myb and hematopoietic stem cells. Science. 2012; 336:86–90. [PubMed: 22442384]

Schwab SR, Cyster JG. Finding a way out: lymphocyte egress from lymphoid organs. Nat Immunol. 2007; 8:1295–1301. [PubMed: 18026082]

Shi C, Pamer EG. Monocyte recruitment during infection and inflammation. Nat Rev Immunol. 2011; 11:762–774. [PubMed: 21984070]

Sipahi I, Debanne SM, Rowland DY, Simon DI, Fang JC. Angiotensin-receptor blockade and risk of cancer: meta-analysis of randomised controlled trials. Lancet Oncol. 2010; 11:627–636. [PubMed: 20542468]

Steidl C, Lee T, Shah SP, Farinha P, Han G, Nayar T, Delaney A, Jones SJ, Iqbal J, Weisenburger DD, Bast MA, Rosenwald A, Muller-Hermelink HK, Rimsza LM, Campo E, Delabie J, Braziel RM, Cook JR, Tubbs RR, Jaffe ES, Lenz G, Connors JM, Staudt LM, Chan WC, Gascoyne RD. Tumor-associated macrophages and survival in classic Hodgkin's lymphoma. N Engl J Med. 2010; 362:875–885. [PubMed: 20220182]

Swirski F, Nahrendorf M, Etzrodt M, Wildgruber M, Cortez-Retamozo V, Panizzi P, Figueiredo JL, Kohler RH, Chudnovskiy A, Waterman P, Aikawa E, Mempel TR, Libby P, Weissleder R, Pittet M. Identification of splenic reservoir monocytes and their deployment to inflammatory sites. Science. 2009; 325:612–616. [PubMed: 19644120]

Taguchi A, Politi K, Pitteri SJ, Lockwood WW, Faca VM, Kelly-Spratt K, Wong CH, Zhang Q, Chin A, Park KS, Goodman G, Gazdar AF, Sage J, Dinulescu DM, Kucherlapati R, Depinho RA, Kemp CJ, Varmus HE, Hanash SM. Lung cancer signatures in plasma based on proteome profiling of mouse tumor models. Cancer Cell. 2011; 20:289–299. [PubMed: 21907921]

Tsubakimoto Y, Yamada H, Yokoi H, Kishida S, Takata H, Kawahito H, Matsui A, Urao N, Nozawa Y, Hirai H, Imanishi J, Ashihara E, Maekawa T, Takahashi T, Okigaki M, Matsubara H. Bone marrow angiotensin AT1 receptor regulates differentiation of monocyte lineage progenitors from hematopoietic stem cells. Arterioscler Thromb Vasc Biol. 2009; 29:1529–1536. [PubMed: 19628784]

Ugel S, Peranzoni E, Desantis G, Chioda M, Walter S, Weinschenk T, Ochando JC, Cabrelle A, Mandruzzato S, Bronte V. Immune Tolerance to Tumor Antigens Occurs in a Specialized Environment of the Spleen. Cell Rep AOP. 2012

van Furth R, Cohn ZA. The origin and kinetics of mononuclear phagocytes. J Exp Med. 1968; 128:415–435. [PubMed: 5666958]

Weissleder R, Pittet MJ. Imaging in the era of molecular oncology. Nature. 2008; 452:580–589. [PubMed: 18385732]

Wilop S, von Hobe S, Crysandt M, Esser A, Osieka R, Jost E. Impact of angiotensin I converting enzyme inhibitors and angiotensin II type 1 receptor blockers on survival in patients with advanced non-small-cell lung cancer undergoing first-line platinum-based chemotherapy. J Cancer Res Clin Oncol. 2009; 135:1429–1435. [PubMed: 19399518]

Wright DE, Wagers AJ, Gulati AP, Johnson FL, Weissman IL. Physiological migration of hematopoietic stem and progenitor cells. Science. 2001; 294:1933–1936. [PubMed: 11729320]

Zhang B, Yao G, Zhang Y, Gao J, Yang B, Rao Z, Gao J. M2-Polarized tumor-associated macrophages are associated with poor prognoses resulting from accelerated lymphangiogenesis in lung adenocarcinoma. Clinics (Sao Paulo). 2011a; 66:1879–1886. [PubMed: 22086517]

Zhang BC, Gao J, Wang J, Rao ZG, Wang BC, Gao JF. Tumor-associated macrophages infiltration is associated with peritumoral lymphangiogenesis and poor prognosis in lung adenocarcinoma. Med Oncol. 2011b; 28:1447–1452. [PubMed: 20676804]

Zitvogel L, Apetoh L, Ghiringhelli F, Kroemer G. Immunological aspects of cancer chemotherapy. Nat Rev Immunol. 2008; 8:59–73. [PubMed: 18097448]

HIGHLIGHTS

- AngII-AGTR1A signaling promotes splenic amplification of macrophage progenitors.
- AngII retains HSCs and macrophage progenitors in spleen by repressing $S1P_1$ sensing.
- Mouse NSCLC exploits the AngII pathway to amplify the macrophage response.
- Controlling AngII production restrains tumor-promoting macrophage response in mice.

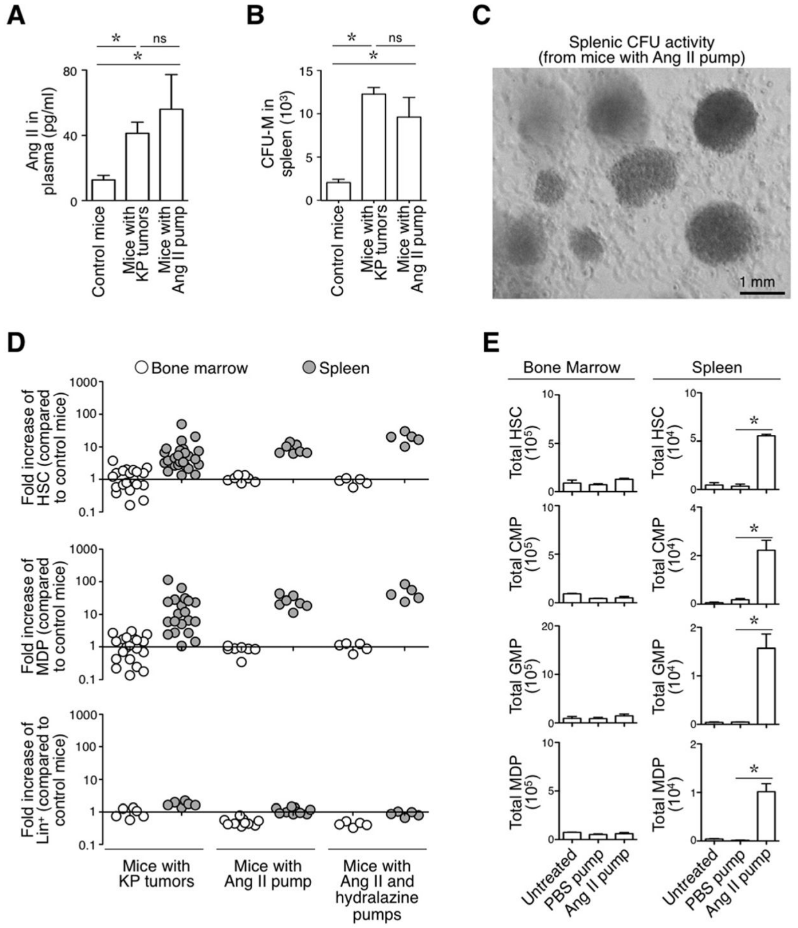

Figure 1. (See also Figure S1). AngII amplifies HSC and macrophage progenitors in the spleen regardless of hemodynamics

A. AngII concentration in plasma (measured by ELISA) from control mice (n=9), mice with KP tumors at 11–12 wk post tumor initiation (n=12) and mice infused with AngII via an osmotic mini-pump (n= 6).

B. Number of colony-forming units (CFUs) obtained with total splenocytes from control mice (n=3), mice with KP tumors (n=3) and mice infused with AngII (n=4).

C. Representative photograph of CFUs obtained with splenocytes from a mouse infused with AngII. Scale bar represents 1 mm.

D. Fold increase in the number of HSCs (top), MDPs (middle) and Lin^+ cells (down) in bone marrow (white circles) and spleen (gray circles) of KP mice (n=27), mice with AngII pump (n=6) and mice with AngII and hydralazine pumps (n=5), when compared to untreated control mice (average from n=5–12). (Lin defined as [B220/CD19/CD90.2/DX5/NK1.1/Ly-6G]).

E. Quantification of HSCs, CMPs, GMPs and MDPs in the bone marrow (left) and spleen (right) of mice that were left untreated (Control, n=5), that received a mini-pump delivering PBS for 8 d (PBS pump, n= 5) and that received a mini-pump delivering AngII for 8 d (AngII pump, n=5).

Data in A, B and E are presented as mean ± SEM. Data in E indicate measurements for single mice. *, $p<0.05$; ns, non-significant.

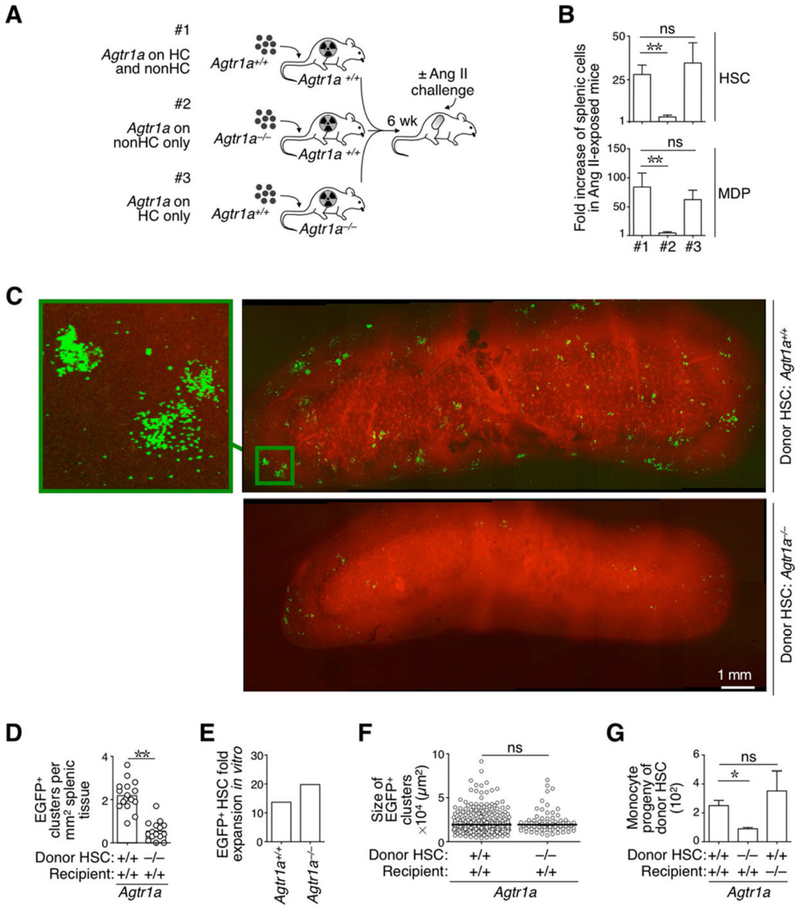

Figure 2. (See also Figure S2). AngII amplifies HSCs and macrophage progenitors via direct signaling through the AGTR1A receptor

A. Cartoon depicting the generation of three different bone marrow chimeras and their use in experiments. #1: reconstituted mice express the *Agtr1a* receptor on hematopoeitic cells (HC) and on non-HC; #2: reconstituted mice express the *Agtr1a* receptor on non-HC only and #3: reconstituted mice express the *Agtr1a* receptor on HC only. All mice were challenged with AngII *in vivo* (delivered via a mini-pump) before examination of the hematopoietic response.

B. Fold increase in the number of splenic HSCs (top) and MDPs (bottom) in AngII-treated mice in groups #1, #2 and #3 (as described in panel A; n=3–4) and when compared to untreated control mice (average from n=4).

C. Intravital micrographs of the splenic red pulp from mice that received *Agtr1a*$^{+/+}$ (top) or *Agtr1a*$^{-/-}$ (bottom) EGFP^{+} HSCs. Left image on top shows *Agtr1a*$^{+/+}$ HSC-derived cell clusters at higher magnification. Venous sinuses are in red. Data are representative of 2 mice per condition analyzed. Scale bar represents 1 mm.

D. Number of EGFP^{+} clusters per mm^{2} of splenic tissue from mice described in panel C.

E. Fold expansion of *Agtr1a*$^{-/-}$ and *Agtr1a*$^{+/+}$ HSCs *in vitro* upon culture for 3 d in complete HSC medium.

F. Size of EGFP^{+} clusters in splenic tissue from mice described in panel C.

G. Tracking of monocyte-derived HSCs *in vivo*. Recipient mice were exposed to AngII and received an i.v. injection of EGFP^{+} HSCs. The monocyte progeny was quantified 5 d later by flow cytometry. Donor HSCs and recipient mice were either *Agtr1a*$^{-/-}$ or *Agtr1a*$^{+/+}$ as indicated.

Data are presented as mean ± SEM. *, $p<0.05$; **, $p<0.01$; ns, non-significant.
See also Fig S2.

NIH-PA Author Manuscript NIH-PA Author Manuscript NIH-PA Author Manuscript

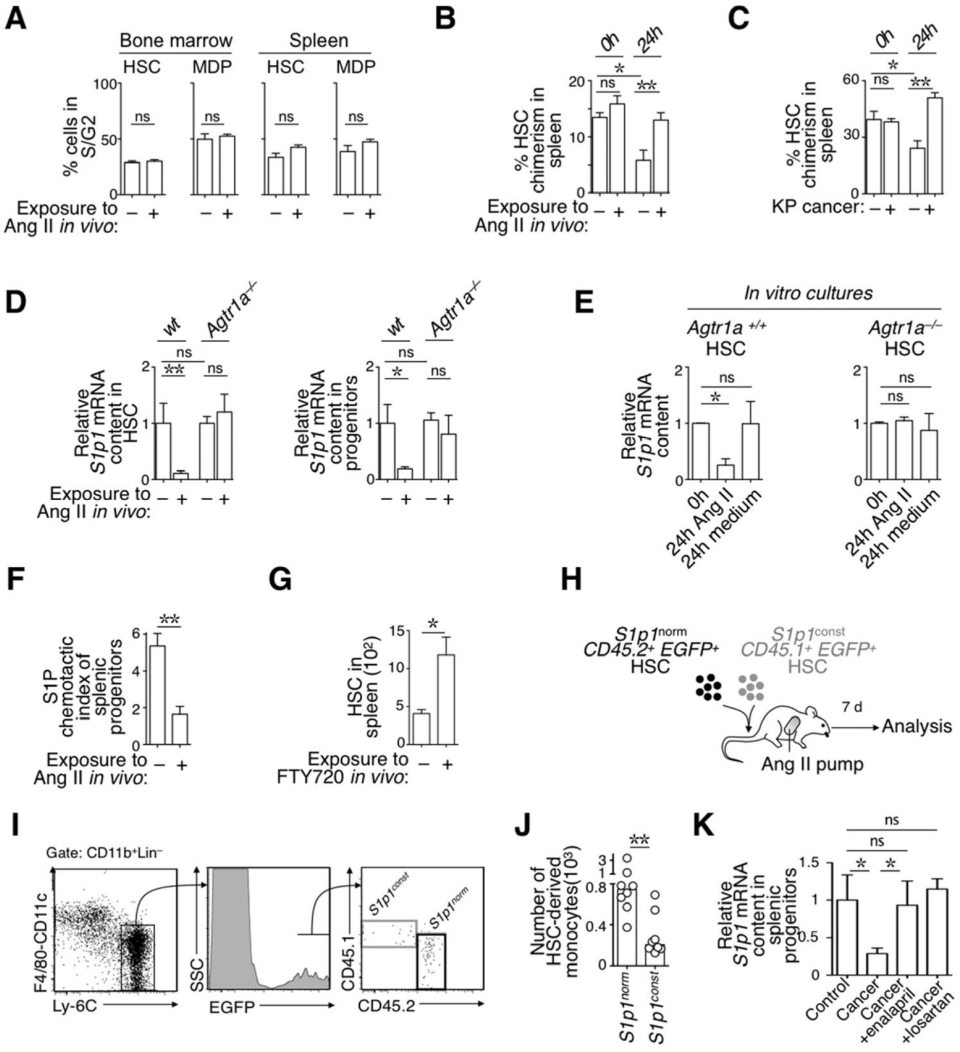

Figure 3. (See also Figure S3). AngII signaling retains HSCs in the spleen in a S1P$_1$-dependent manner

A. Percent of bone marrow (left) and splenic (right) HSC and MDP populations in S/G2 phase of the cell cycle. Cells were obtained from mice treated (+AngII, n=4) or not (Control, n=3) with AngII for 1 wk, stained with DAPI *ex vivo* and analyzed immediately by flow cytometry.

B. Percent chimerism of splenic HSCs in mice parabiosed for 14 d, with each of the parabionts either infused, or not, with AngII. Data show chimerism at the time of separation (0h, n=2) and 1 d later (24h, n=4).

C. Percent chimerism of splenic HSCs in mice parabiosed for 30 d, with each of the parabionts bearing KP tumors (+ KP cancer) or not (− KP cancer). Data show chimerism at the time of separation (0h, n=4) and 1 d later (24h, n=4).

D. Relative *S1p1* mRNA content in splenic HSCs (left) and macrophage progenitors (right) obtained from *Agtr1a*$^{+/+}$ or *Agtr1a*$^{-/-}$ mice. Mice were exposed or not to AngII *in vivo* for 1 wk, as indicated, and analyzed immediately *ex vivo* (n=6–7). Values are normalized to *S1p1* mRNA expression in wild-type cells obtained from untreated mice (average from n=6).

E. Relative *S1p1* mRNA expression levels in *Agtr1a*$^{+/+}$ (left) and *Agtr1a*$^{-/-}$ HSCs analyzed immediately (0h, n=2) and after 24h in medium supplemented with 10 μM AngII (24h AngII, n=3); or after 24h in medium alone (24h medium, n=3).

NIH-PA Author Manuscript NIH-PA Author Manuscript NIH-PA Author Manuscript

F. *Ex vivo* chemotactic index of splenic Lin$^-$ CD117$^+$ progenitor cells toward an S1P gradient. Cells were obtained from mice exposed, or not, to AngII *in vivo* (n=4). (Lin defined as [B220/CD19/CD90.2/DX5/NK1.1/Ly-6G/CD11b/CD11c]).

G. Accumulation of splenic HSCs in animals that received i.p. injections of PBS (−FTY720) or FTY720 (+FTY720) for 7 consecutive days (n=5).

H. Procedure used to co-inject equal numbers of *S1p1*^{norm} and *S1p1*^{const} HSC populations. The progeny of each HSC population was evaluated 7 d later.

I. Detection by flow cytometry of the progeny of CD45.2 *S1p1*^{norm} and CD45.1 *S1p1*^{const} HSCs. HSC-derived monocytes were defined as CD11b$^+$ Lin$^-$ [F4/80/ CD11c]^{lo} Ly-6C^{hi} EGFP$^+$ (Lin: [B220/ CD19/ CD90.2/ DX5/ NK1.1/ Ly-6G]).

J. Quantification of *S1p1*^{norm} and *S1p1*^{const} HSC-derived monocytes (n=8) in mice described in panel I.

K. Relative *S1p1* mRNA content in splenic progenitors obtained from tumor-free mice (control, n=10), KP mice at wk 12 post tumor initiation (KP, n=10), KP mice that were treated with enalapril for 12 d (KP +enalapril, n=10), and KP mice that were treated with losartan for 7 d (KP +losartan, n=4).

Data are presented as mean ± SEM. *, p<0.05; **, p<0.01; ns, non-significant.

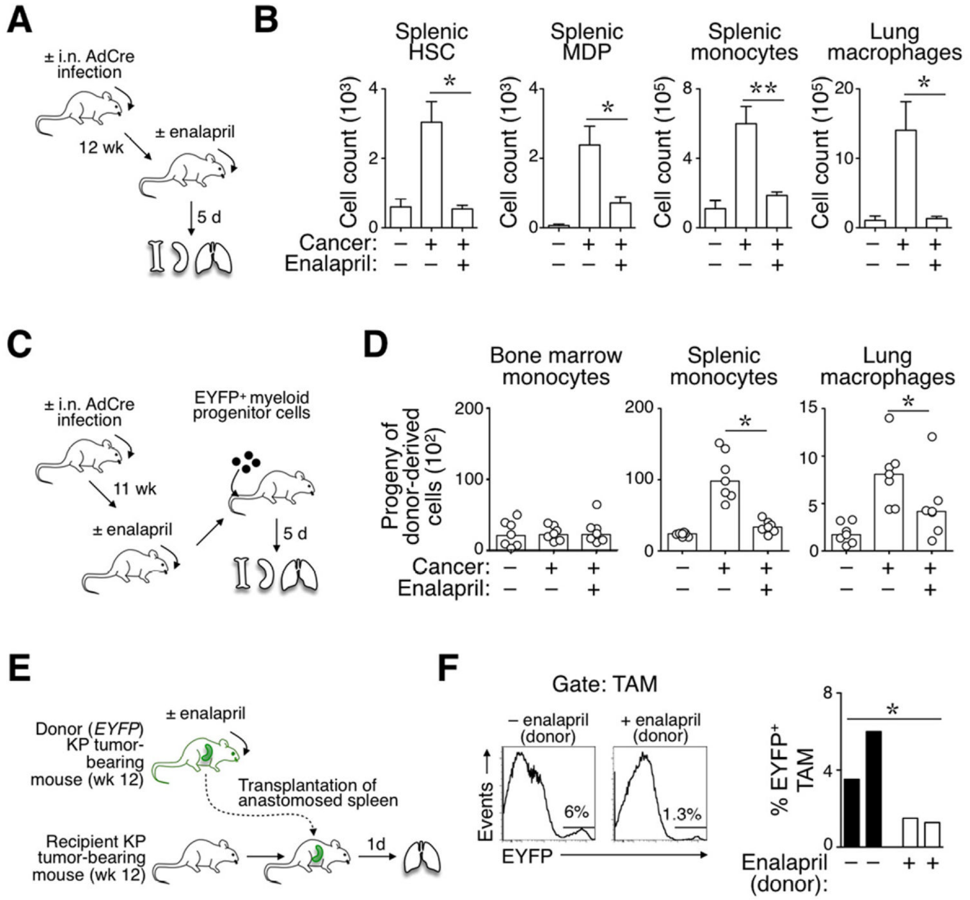

Figure 4. (See also Figure S4). Reduction of AngII production impairs the TAM response at its source

A. Procedure used to measure the effects of short-term enalapril administration on splenic and lung responses in mice treated or not for 5 d with enalapril (treatment was initiated 12 wk post tumor initiation). Age-matched, tumor-free untreated mice served as controls

B. Quantification of splenic HSCs, MDPs, monocytes and lung macrophages in the cohorts of mice described in panel A (n≥4).

C. Procedure used to track the progeny of $EYFP^+$ myeloid progenitor cells transferred into mice with or without lung cancer (±AdCre infection) and treated or not with enalapril. The $EYFP^+$ progenitor cells were injected 11 wk post tumor initiation. The progeny of these cells was evaluated in bone marrow, spleen and lung 5 d later.

D. Number of $EYFP^+$ myeloid progenitor-derived monocytes (in bone marrow and spleen) and macrophages (in lungs) in mice described in panel C (n=6–7).

E. Procedure used to transplant spleens from donor KP mice (treated or not with enalapril) into recipient KP mice (not treated with enalapril).

F. Top: Flow cytometry histogram profiles show donor spleen-derived $EYFP^+$ TAMs that accumulated in the lungs of recipient KP mice (experimental procedure described in panel E). The transplanted spleens were obtained from mice that were previously treated or not with enalapril (±enalapril (donor)). Bottom: Quantification of $EYFP^+$ TAMs derived from donor spleens that were treated (white bars) or not (black bars) with enalapril. Recipient mice were sacrificed and analyzed 1 d post transplantation (n=2).

Data in B are presented as mean ± SEM. Data in D are presented as median with dots indicating measurements for single mice. *, $p<0.05$; **, $p<0.01$; ns, non-significant.

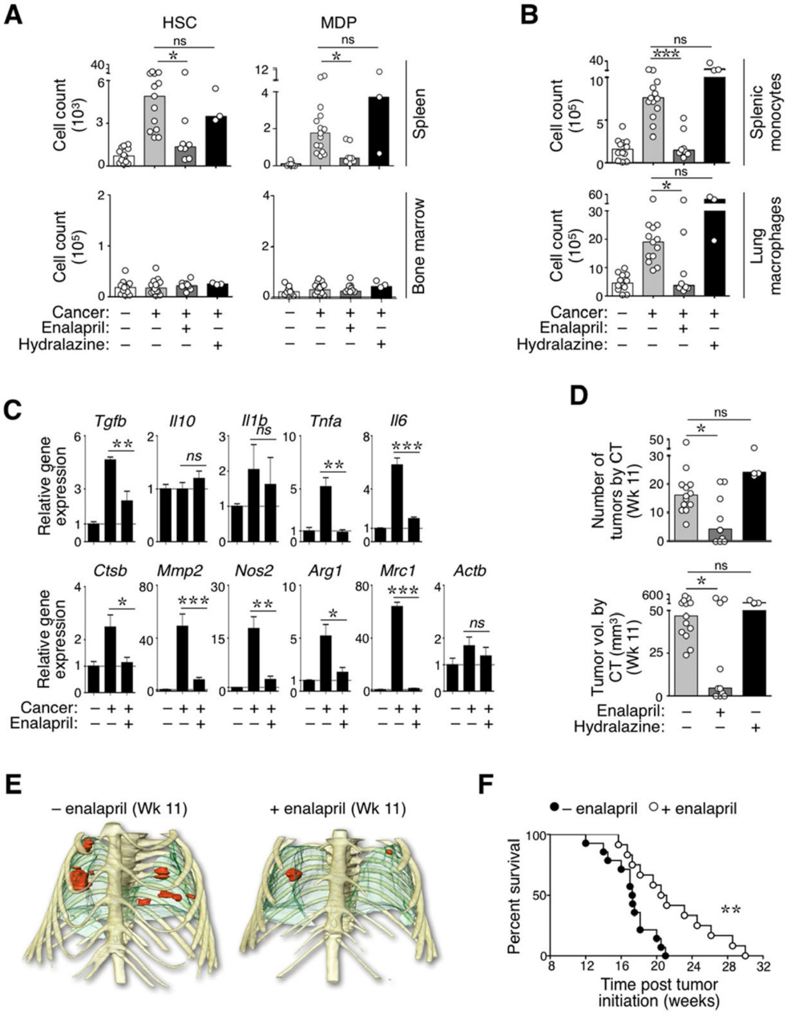

Figure 5. (See also Figure S5): Prolonged reduction of AngII production restrains the tumor-promoting TAM response and delays tumor mortality in KP mice

A. Quantification of splenic and bone marrow-derived HSCs and MDPs in four cohorts of mice. From left to right: age-matched control mice (−cancer, n=13); tumor-bearing KP mice (+cancer, n=13), KP mice treated with enalapril (+Cancer +enalapril; n=8) and KP mice treated with hydralazine (+cancer +hydralazine; n=3). Tumor-bearing mice were analyzed at 11 wk post tumor initiation. Administration of enalapril or hydralazine started at wk 8.

B. Quantification of splenic monocytes (top) and lung macrophages (bottom) in the same mice as in A.

C. Phenotypic characterization of lung macrophages. F4/80^{+} CD11c$^{int/+}$ Lin^{-} macrophages (Lin defined as [B220/CD19/CD90.2/DX5/NK1.1/Ly-6G]^{lo}) were isolated from lungs of control mice (−cancer), tumor-bearing KP mice (+cancer) and tumor-bearing KP mice treated with enalapril (+cancer +enalapril). Mice were analyzed at 11 wk post tumor initiation. Treatment with enalapril started at wk 8. Data show relative mRNA expression levels (real time PCR) normalized to 18s rRNA. Analysis of *Actb* (Actin-b) expression was included as an internal control.

D. Number (top) and total volume (bottom) of lung tumors detected by high resolution CT at 11 wk post tumor initiation in KP mice. The legend identifies mice that started a treatment with enalapril or hydralazine at wk 8.

E. Representative 3D volume renderings of tumors at week 11 (Wk 11) from mice treated (bottom) or not (top) with enalapril for 3 consecutive weeks. Tumors are shown in red, lungs in green and bones in yellow.

F. Kaplan-Meier survival analysis of KP mice treated (n=12) or not (n=14) with enalapril starting at wk 8 post tumor initiation.

Data in A–B and D are presented as median with dots indicating measurements for single mice. Data in C are presented as mean ± SEM. *, $p<0.05$; **, $p<0.01$, ***, $p<0.001$; ns, non-significant.

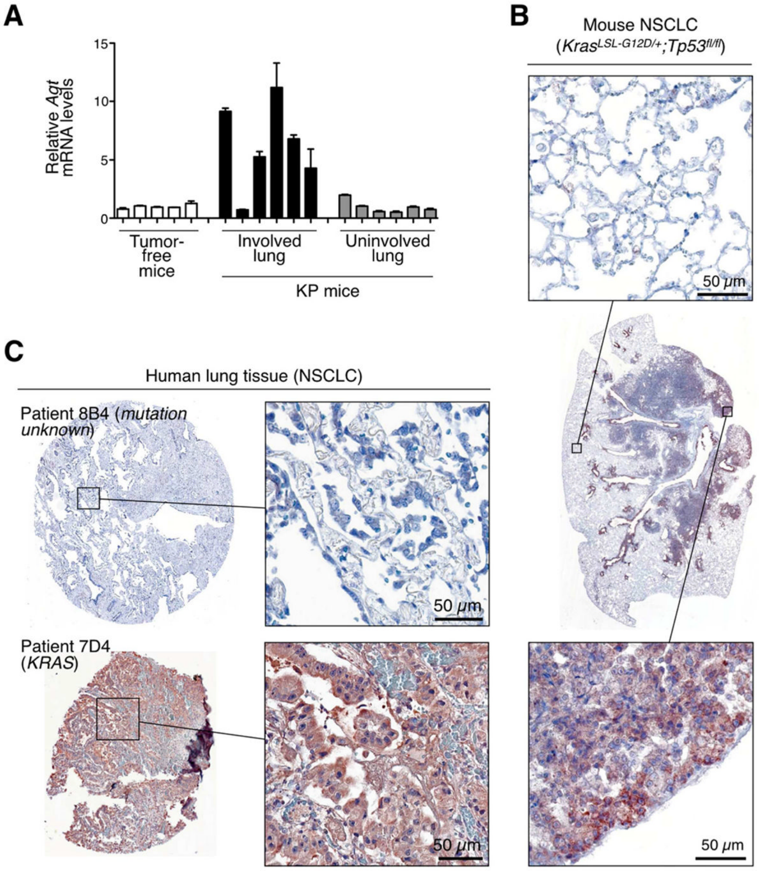
A
Relative Agt mRNA levels
15
10
5
0
Tumor-free mice
Involved lung
Uninvolved lung
KP mice
B
Mouse NSCLC
($Kras^{LSL\text{-}G12D/+}$;$Tp53^{fl/fl}$)
50 μm
50 μm
C
Human lung tissue (NSCLC)
Patient 8B4 (mutation unknown)
50 μm
Patient 7D4 (KRAS)
50 μm

Figure 6. (See also Figure S6 and Table S1). Agt over-expression in mouse and a subset of human NSCLC

A. Relative *Agt* mRNA levels in tumor-involved and uninvolved lung tissue of KP mice at 11–12 wk post tumor initiation. Lung tissue of tumor-free mice served as control. mRNA expression is relative to lung tissue of tumor-free mice. Each bar represents a distinct tissue biopsy (n=3 technical replicates per sample).

B. Histological detection of Agt protein in the tumor stroma of KP mice at 11 wk post tumor initiation. Center: full view of the lung lobe; top: higher magnification image of uninvolved tissue; bottom: higher magnification image of tumor-involved tissue. Data are representative of 4 mice. Scale bar represents 50 μm.

C. Representative examples of detectable AGT protein expression (patient 7D4) or absence thereof (patient 8B4) in lung biopsy specimens from a total of 44 patients with stage 1 NSCLC. AGT staining was scored from 0 to 200 as described in Supplementary Materials and Methods (scores for patient 8B4 is 0 and for patient 7D4 is 95). Scale bar represents 50μm. Known genetic alterations (*KRAS)* are indicated.

Data in A are presented as mean ± SEM